Monthly Notices of the ROYAL ASTRONOMICAL SOCIETY

MNRAS **448,** 1628–1633 (2015) doi:10.1093/mnras/stv056

Stellar wind erosion of protoplanetary discs

N. R. Schnepf,[1]★ R. V. E. Lovelace,[2] M. M. Romanova[2] and V. S. Airapetian[3]

[1]*Earth, Atmospheric and Planetary Sciences, MIT, Cambridge, MA 02139, USA*
[2]*Department of Astronomy, Cornell University, Ithaca, NY 14853, USA*
[3]*NASA/Goddard Space Flight Center, Greenbelt, MD 20771, USA*

Accepted 2015 January 8. Received 2014 December 31; in original form 2014 May 21

ABSTRACT

An analytic model is developed for the erosion of protoplanetary gas discs by high-velocity magnetized stellar winds. The winds are centrifugally driven from the surface of rapidly rotating, strongly magnetized young stars. The presence of the magnetic field in the wind leads to Reynolds numbers sufficiently large to cause a strongly turbulent wind/disc boundary layer which entrains and carries away the disc gas. The model uses the conservation of mass and momentum in the turbulent boundary layer. The time-scale for significant erosion depends on the disc accretion speed, disc accretion rate, the wind mass-loss rate, and the wind velocity. The time-scale is estimated to be $\sim 2 \times 10^6$ yr. The analytic model assumes a steady stellar wind with mass- loss rate $\dot{M}_{\rm w} \sim 10^{-10}\,{\rm M}_\odot\ {\rm yr}^{-1}$ and velocity $v_{\rm w} \sim 10^3$ km s^{-1}. A significant contribution to the disc erosion can come from frequent powerful coronal mass ejections (CMEs) where the average mass-loss rate in CMEs, $\dot{M}_{\rm CME}$, and velocities, $v_{\rm CME}$, have values comparable to those for the steady wind.

Key words: accretion, accretion discs – magnetic fields – Sun: coronal mass ejections (CMEs) – stars: pre-main-sequence – stars: winds, outflows.

1 INTRODUCTION

A wide body of observations establish that the lifetime of gaseous protoplanetary discs is relatively short. While most protostars younger than 10^6 yr have gaseous discs, only 50 per cent of protostars 3×10^6 yr in age have gaseous discs and very few stars 6×10^6 yr or older have gaseous discs (Armitage 2010). From spectroscopic observations of the hot continuum radiation produced when infalling gas impacts the stellar surface, it is known that the accretion rate of gas on to a star decays on a similar time-scale (Hartmann et al. 1998). Observations also suggest that the dispersal of gas occurs on a wide range of disc radii during a short time-scale (Skrutskie et al. 1990; Wolk & Walter 1996; Andrews & Williams 2005).

The short lifetime of a gaseous disc plays a critical role in the formation of planetary systems. It directly affects the time available for planetesimals to agglomerate additional material, as well as the migration of planets within the disc (Armitage 2010; Zsom et al. 2010). The mechanisms by which the gas is lost may play an important role in the formation of planetary systems.

A class of protoplanetary discs termed *transition discs* have been identified by a dip in the mid-infrared spectra which can be modelled by a reduced surface density of dust in the inner regions ($\lesssim$35 au) of the discs (Espaillat et al. 2007, 2014). Submillimetre imaging directly shows a deficit in surface density of dust in these systems (e.g. Piétu et al. 2006). The observations suggest an inside-out dispersal of the dust possibly caused by photoevaporation (Clarke, Gendrin & Sotomayor 2001; Owen, Clarke & Ercolano 2012), by the presence of giant planets, or other processes (Birnstiel et al. 2013). Photoevaporative destruction of discs is thought to occur when the photoevaporative mass-loss rate $\dot{M}_{\rm pe}$ exceeds the accretion rate $\dot{M}_{\rm d}$ on to the star (e.g. Richling & Yorke 1997; Hollenbach, Yorke & Richstone 2000). Additionally, the radial distribution of dust is influenced by grain growth, migration, destruction in collisions, and trapping in vortices excited at the outer gap edge caused by giant planets (Regály et al. 2012). Transition discs have lower accretion rates than younger standard discs, but not sufficiently low to explain the large sizes of the regions of low dust density by photoevaporation (Birnstiel 2013). A promising possibility is that the depletion of dust in the inner regions of transitional disc is due to the presence of multiple planets located at radii $\sim$0.1–10 au (Espaillat et al. 2014).

Multiple processes may be responsible for the loss of the gas and entrained dust from protoplanetary discs. This work analyses the erosion of the gas and entrained dust particles from discs caused by high-velocity magnetized stellar winds. The presence of the magnetic field leads to Reynolds numbers sufficiently large to cause a strongly turbulent wind and disc boundary layer (see Fig. 1) as suggested by Lovelace, Romanova & Barnard (2008). Strong magnetized winds from young stars with discs are likely because the stars are known to rotate rapidly and to be strongly magnetized.

★ E-mail: nschnepf@mit.edu

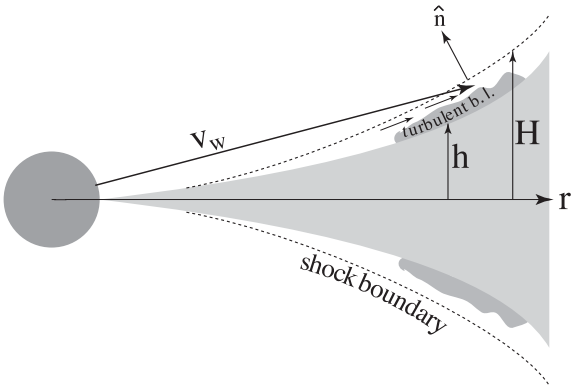

Figure 1. A cross-section of the protoplanetary disc with the disc–wind turbulent boundary layer ($h < z < H$) and outer oblique shock shown. $\hat{\boldsymbol{n}}$ is the normal to the shock wave, $\boldsymbol{v}_{\rm w}$ is the wind velocity, h is the disc half-thickness, and H is the vertical height of the shock. The figure has been adapted from a figure in Lovelace et al. (2008).

The magnetic winds depend on both the star's rotation rate *and* its magnetic field owing to complex and likely random dynamo processes. Thus, a one-to-one correlation with the rotation rate is not expected. Wind erosion of protostellar discs has been discussed in a number of previous works as reviewed by Hollenbach et al. (2000). However, the important role played by a rapidly rotating star's magnetic field in launching a high-velocity wind has apparently not been considered. Furthermore, the role of the wind's magnetic field in producing a strongly turbulent wind/disc boundary layer has not been discussed. In addition to a steady high-velocity stellar wind, we consider the disc erosion due to frequent powerful coronal mass ejections (CMEs).

Section 2 of the paper discusses magnetized stellar winds. Section 3 develops an analytic model for the evolution of the mass surface density of the disc $\Sigma_{\rm d}(r, t)$. Section 4 discusses the contribution to disc erosion resulting from frequent powerful CMEs. Section 5 gives the conclusions of this work.

2 MAGNETIZED STELLAR WINDS

The winds from rotating magnetized stars may be thermally driven as in the solar wind. The magnetic field has an important role in the outward transport of angular momentum by the wind (Weber & Davis 1967; Matt & Pudritz 2008a,b). For thermally driven winds from slowly rotating stars, the radial flow velocity at large distances is the Parker velocity $v_{\rm P} = [2c_{\rm s0}^2/(\gamma - 1) - 2\,GM_*/R_*]^{1/2}$, where $c_{\rm s0}$ is the sound speed at the star's radius R_*, M_* is its mass, and γ is the specific heat ratio. [Note that both spherical (R, θ, ϕ) and cylindrical (r, ϕ, z) inertial coordinates are used in this work.]

In contrast, for conditions where (1) the thermal speed of the gas close to the star is small (compared with the velocity), (2) the star's magnetic field is strong, and (3) the star rotates rapidly, there are magnetically driven winds (also termed fast magnetic rotator, FMR, winds; Michel 1969; Belcher & MacGregor 1976). These winds are driven by the centrifugal force of the star's rapidly rotating magnetic field rather than the thermal energy in the star's corona.

For a rotating magnetized star, the radial wind velocity at large distances from the star is $v_{\rm w} = 1.5[\Omega_*^2(B_{R*}R_*^2)^2/\dot{M}_{\rm w}]^{1/3}$ (Michel 1969), where $P_* = 2\pi/\Omega_*$ is the rotation period of the star and $B_{R*} = B_R(R_*)$. The characteristic acceleration distance of the winds is the Alfvén radius of the wind, $R_{\rm Aw} = (2/3)^{1/2}(v_{\rm w}/\Omega_*)$ (Belcher & MacGregor 1976). For a star with rotation period $P_* = 10\,$d, a radius twice the radius of the Sun, $R_* = 1.4 \times 10^{11}$ cm (Armitage & Clarke 1996), a surface magnetic field $B_{R*} = 0.5$ kG, and $\dot{M}_{\rm w} = 10^{-10}\,{\rm M}_\odot\,{\rm yr}^{-1}$, one finds $v_{\rm w} \approx 1400\,{\rm km\,s}^{-1}$, and $R_{\rm Aw} \approx 1$ au. For the magnetic acceleration of the solar wind to be important, the product of the rotation rate Ω_* times the magnetic flux per sterradian $B_{R*}R_*^2$ would need to be $\sim$20 times larger than the present values (Belcher & MacGregor 1976). The magnetic winds cause the rapid spin-down of the stars on a time-scale $T_{\rm sdw} = I[(2/3)R_{\rm Aw}^2\dot{M}_{\rm w}]^{-1}$, where I is the moment of inertia of the star (Weber & Davis 1967; Belcher & MacGregor 1976). This time-scale may be as short as $\sim 10^6$ yr. However, the spin-down torque of the wind is strongly dominated by the spin-up torque due to the disc accretion to the star for accretion rates $\sim 10^{-8}\,{\rm M}_\odot\,{\rm yr}^{-1}$. In this regime, the star's rotation tends to be locked to the rotation rate of the inner disc by the magnetic coupling between the star and the disc as proposed by Königl (1991) and observed in magnetohydrodynamic (MHD) simulations by Long, Romanova & Lovelace (2005). In contrast, Matt & Pudritz (2008a,b) argue theoretically that the magnetic coupling is ineffective and that an accretion powered stellar wind acts to counteract the tendency of the accretion to spin-up the star. A review of this topic is given by Bouvier et al. (2014).

The magnetic fields of classical T Tauri stars (CTTSs) are typically in the kG range (Johns-Krull & Valenti 2000; Johns-Krull 2007). Furthermore, these stars typically rotate rapidly with periods $\sim$2–15 d (Bouvier et al. 1993, 2014). Thus, magnetically driven winds may be important for T Tauri stars.

Magnetically driven winds from the disc/magnetospheric boundary have been found in MHD simulations of rapidly rotating, disc-accreting stars particularly in the 'propeller'regime (Romanova & Bisnovatyi-Kogan 1999; Romanova et al. 2005, 2009; Ustyugova et al. 2006; Lovelace, Lii, Romanova & Lovelace 2012; Lii et al. 2014). The propeller regime arises when the magnetospheric radius $r_{\rm m}$ becomes larger than the corotation radius $r_{\rm cr} = (GM_*/\Omega_*^2)^{1/3}$. Because $r_{\rm m}$ depends inversely on the disc accretion rate $\dot{M}_{\rm a}$ (to a fractional power), the propeller regime is unavoidable as $\dot{M}_{\rm a}$ decreases in the late stages of disc evolution. The winds are found to flow in opposite directions along the rotation axis transporting energy and angular momentum away from the star. For the case of an aligned a dipole field, the field acts to block an equatorial outflow. However, for multipolar fields, winds are expected in all directions from the star's surface.

In deriving the evolution of disc density due to this magnetized wind, it is useful to consider the physical conditions in the wind at a distance from the sun of $R = 1$ au with fiducial conditions of wind density $n_{\rm w} = 10^5\,{\rm cm}^{-3}$, wind speed $v_{\rm w} = 10^3\,{\rm km\,s}^{-1}$, a predominantly toroidal time averaged magnetic field $B_{\rm w} = 0.1$ G, and ion (proton) and electron temperatures of $T_{\rm i} = T_{\rm e} = 10^5$ K. From this distance and beyond, (1) the wind velocity is predominantly radial, (2) it is superfast magnetosonic, and (3) it is much larger than the Keplerian velocity of the disc matter.

Under these conditions, the ion and electron gyrofrequencies are $\omega_{ci} \approx 10^3\ {\rm s}^{-1}$ and $\omega_{ce} \approx 2 \times 10^6\ {\rm s}^{-1}$. The corresponding ion and electron gyroradii are $r_{\rm gi} \approx 3 \times 10^3$ cm and $r_{\rm ge} \approx 70$ cm. From this, the ion and electron collision times ($\propto T^{3/2}/n$) are $\tau_{\rm i} \approx 470$ s and $\tau_{\rm i} \approx 11$ s. The ion and electron mean-free paths are $\ell_{\rm i} = \ell_{\rm e} = 1.4 \times 10^9$ cm (Braginskii 1965). Thus, $\omega_{ci}\tau_{\rm i} \approx 4.6 \times 10^5$ and $\omega_{ce}\tau_{\rm e} \approx 2 \times 10^7$.

In the absence of a magnetic field, the kinematic viscosities of ions and electrons are $\nu_{0\rm i} \approx v_{\rm thi}^2\tau_{\rm i} \approx 4 \times 10^{15}\ {\rm cm}^2\ {\rm s}^{-1}$ and $\nu_{0\rm e} \approx v_{\rm the}^2\tau_{\rm e} \approx 2 \times 10^{17}\ {\rm cm}^2\ {\rm s}^{-1}$, where $v_{\rm th,\,i,\,e}$ is the ion or electron thermal speed. Thus, without a magnetic field the Reynolds

number, $\mathrm{Re} = rv_\mathrm{w}/\nu_{0\mathrm{e}} \approx 9000$, is such that a boundary layer flow is laminar.

When the magnetic field is included, there are five different viscosity coefficients. Fortunately, for the considered problem the important viscosity coefficient is that for momentum transport across the magnetic field. For example, the momentum flux-density component is $T_{R\theta} = -\rho\nu_\perp R^{-1}\partial v_R/\partial\theta$. For ions, the viscosity term is $\nu_{\perp\mathrm{i}} \approx \nu_{0\mathrm{i}}/(\omega_{c\mathrm{i}}\tau_\mathrm{i})^2 \approx 2\times10^4$ cm^2 s^{-1}, and for electrons it is $\nu_{\perp\mathrm{e}} \approx \nu_{0\mathrm{e}}/(\omega_{c\mathrm{e}}\tau_\mathrm{e})^2 \approx 500$ cm^2 s^{-1}. Using the viscosity $\nu_{\perp\mathrm{i}}$, the effective Reynolds number for the wind is $\mathrm{Re}_\mathrm{w} = Rv_\mathrm{w}/\nu_{\perp\mathrm{i}} \sim 10^{18}$. Evidently, unlike the non-magnetic case with laminar boundary layer flow, with a magnetic field the boundary layer flow is strongly turbulent. The large reduction of the viscosity results from the particle step size between collisions being a gyroradius rather than a mean-free path. Thus, the estimated Reynolds number also holds for a turbulent magnetic field.

The relevant heat conductivity coefficient is that for the heat flux across the magnetic field, $q_\theta = -\kappa_\perp R^{-1}\partial(k_B T)/\partial\theta$, where $\kappa_\perp \approx \kappa_{\perp\mathrm{i}} \approx 2nv_{\mathrm{thi}}^2\tau_\mathrm{i}/(\omega_{c\mathrm{i}}\tau_\mathrm{i})^2 \approx 3.8\times10^9$ (cm s)$^{-1}$ and where k_B is Boltzman's constant. For this heat conductivity, the heat flow from the wind into the disc is negligible compared with the energy flux per unit area from the disc $[3GM_*\dot{M}_\mathrm{d}/(8\pi R^3)]$ for accretion rates $\dot{M}_\mathrm{d} \sim 10^{-8}$ M$_\odot$ yr^{-1}, which is in turn small compared to the irradiation of the disc by the star.

A weak oblique shock arises where the wind encounters the much denser disc. This occurs at a height $H(r) \ll r$ above the equatorial plane for a disc with half-thickness $h(r) < H(r)$ (Fig. 1). The angle between the incident flow and the shock is $\beta \approx r\mathrm{d}(H/r)/\mathrm{d}r \ll 1$, with β expected to be >0.

After passing through the shock, the flow is deflected by an angle $\delta = 2\beta/(1+\gamma) = 3\beta/4$ (where $\gamma = 5/3$) away from the equatorial plane, and the flow speed is reduced by a small fractional amount. This region between h and H is the boundary layer. The influx of wind matter into this layer is $-\mathrm{d}\boldsymbol{S}\cdot(\rho_\mathrm{w}\boldsymbol{v}_\mathrm{w}) \approx \mathrm{d}S\rho_\mathrm{w}v_\mathrm{w}r[\mathrm{d}(H/r)/\mathrm{d}r]$, where $\mathrm{d}S = r\mathrm{d}r\mathrm{d}\phi$ is the area element of the shock on the top side of the disc. The Keplerian velocity ($v_\mathrm{K} = \sqrt{GM/r}$) of the disc is small compared to the wind velocity for $r \geq 1$ au, so it is neglected. The density in the boundary layer varies from $\rho(r,h) \gg \rho_\mathrm{w}$ at the surface of the disc to ρ_w at $z = H$. The time-averaged radial flow velocity varies from $|v_\mathrm{r}(r,h)| \ll v_\mathrm{w}$ to $v_\mathrm{r} = v_\mathrm{w}$ at $z = H$; $v_\mathrm{r}(r,h)$ is neglected.

For an explanation of our notation, it is useful to first consider stationary conditions (later we evaluate the time evolution of the disc). In this case, the conservation of mass and radial momentum in the annular region $a-b-c-d$ (shown in Fig. 2) of the boundary layer on the top side of the disc provides

$$\frac{\partial\left(rF_\mathrm{r}^\mathrm{m}\right)}{\partial r} = r\left[r\frac{\mathrm{d}(H/r)}{\mathrm{d}r}\right]\rho_\mathrm{w}v_\mathrm{w} + \frac{1}{4\pi}\frac{\mathrm{d}\dot{M}_\mathrm{d}}{dr}, \tag{1}$$

$$\frac{\partial\left(rF_\mathrm{r}^\mathrm{p}\right)}{\partial r} = r\left[r\frac{\mathrm{d}(H/r)}{\mathrm{d}r}\right]\rho_\mathrm{w}v_\mathrm{w}^2. \tag{2}$$

The terms on the left-hand side are due to the vertical sides of the region and the right-hand side is due to the sides $a-b$ and $c-d$. Here, F_r^m is the mass flux and F_r^p is the radial momentum flux. Both fluxes are given per unit circumference of the top side of the disc,

$$F_\mathrm{r}^\mathrm{m} = \int_h^H \mathrm{d}z\langle\rho v_\mathrm{r}\rangle, \quad F_\mathrm{r}^\mathrm{p} = \int_h^H \mathrm{d}z\left\langle\rho v_\mathrm{r}^2\right\rangle. \tag{3}$$

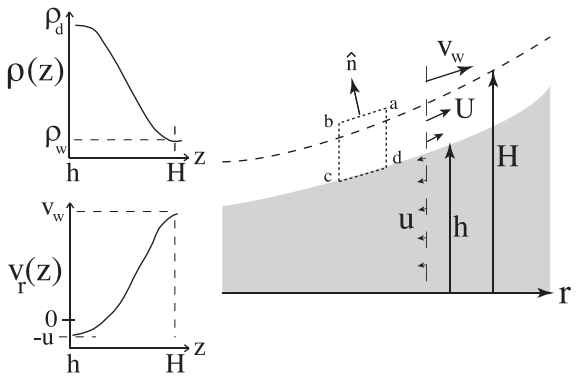

Figure 2. Sketches of the vertical profiles of density ρ and radial velocity $\langle v_\mathrm{r}\rangle$ within the boundary layer is shown on the left. Here, ρ_d is the density at the surface of the disc, ρ_w is the density of the wind, and v_w is the speed of the wind. The figure has been adapted from a figure in Lovelace et al. (2008).

The average radial velocity in the boundary layer is

$$U(r) = \frac{F_\mathrm{r}^\mathrm{p}(r)}{F_\mathrm{r}^\mathrm{m}(r)}. \tag{4}$$

The angular brackets indicate averages are over the turbulent fluctuations. The mass-loss rate of the disc per unit radius due to entrainment is $\mathrm{d}\dot{M}_\mathrm{d}/\mathrm{d}r$. The disc matter influx to the boundary layer brings in negligible radial momentum.

The average velocity U depends on the vertical profiles of density and radial velocity – which are both unknown. We expect the profiles, for example $\langle v_\mathrm{r}(z)\rangle$ to be substantially different from those of laboratory turbulent boundary layers over solid surfaces where $\rho = \mathrm{const}$ (e.g. Schlichting 1968; Roy & Blottner 2006). The main reason for the difference is that the density at the surface of the disc $\rho(r,h)$ is many orders of magnitude larger than the wind density ρ_w. For a laboratory boundary layer, a mixing length model of the momentum transport gives $(z')^2(\mathrm{d}\langle v_\mathrm{r}\rangle/\mathrm{d}z')^2 = \mathrm{const}$, where $z' \equiv z-h$, and this gives the well-known logarithmic velocity profile (see e.g. Schlichting 1968). For this profile most of the change of velocity is quite close to the wall ($z' = 0$). In contrast, for the disc boundary layer a mixing length model gives $\rho(z')(z')^2(\mathrm{d}\langle v_\mathrm{r}\rangle/\mathrm{d}z')^2 = \mathrm{const}$. Because of the density dependence, the change in the velocity occurs relatively far from the wall. An important consequence of this is that the average velocity U is much smaller than v_w, because U is the density weighted average radial velocity. Here, we assume that U is larger by a factor of $g > 1$ than the local escape velocity $v_\mathrm{esc} = (2GM_*/r)^{1/2}$ so that the matter flow in the boundary layer escapes the star.

3 NON-STATIONARY EVOLUTION

In the absence of wind erosion, conservation of the disc matter gives

$$\frac{\partial(2\pi r\Sigma_\mathrm{d})}{\partial t} - \frac{\partial(2\pi ru\Sigma_\mathrm{d})}{\partial r} = 0, \tag{5}$$

where

$$\Sigma_\mathrm{d}(r,t) = \int_{-h}^{h}\mathrm{d}z\ \rho(r,z,t), \quad u(r,t) = -\frac{1}{\Sigma_\mathrm{d}}\int_{-h}^{h}\mathrm{d}z\ \rho v_\mathrm{r}, \tag{6}$$

with $u \geq 0$ being the accretion speed of the disc matter.

For stationary conditions, $ru\Sigma_s = \mathrm{const}$. We assume an α-disc model (Shakura & Sunyaev 1973): $u = \alpha c_\mathrm{s}^2/v_\mathrm{K}$, where $\alpha = \mathrm{const}$

$\sim 10^{-3}$–0.1, c_s is the mid-plane isothermal sound speed, and v_K is the Keplerian velocity of the disc. Commonly considered models have $\Sigma_d \propto r^{-q}$ with $q = \text{const} \sim 1$. This implies that $T \propto r^{q-3/2}$ and $u \propto r^{q-1}$. The disc is assumed to be in hydrostatic equilibrium in the vertical direction so that $h/r = c_s/v_K$ and thus $h/r \propto r^{q/2-1/4}$. For specificity, we adopt $q = 1$ so that $u = \text{const}$ and $h/r \propto r^{1/4}$.

With the wind erosion included, we consider that u and h/r are the same as in a stationary disc in the region where $\Sigma_d(rt) > 0$. The basis for this is the assumption of the Shakura & Sunyaev (1973) $\alpha = \text{const}$ model where u and h depend on the mid-plane disc temperature which in turn depends on the stellar irradiation of the disc. Further, we assume that the surface density in the top and bottom boundary layers, $\Sigma_{bl} = 2\int_h^H dz\, \rho$, is much smaller than Σ_d. Mass conservation then gives

$$\frac{\partial\,(2\pi r\,\Sigma_d)}{\partial t} - \frac{\partial\,(2\pi r u\,\Sigma_d)}{\partial r} = -4\pi\frac{\partial\,(r\,F_r^m)}{\partial r} + 4\pi r^2\left[\frac{d}{dr}\left(\frac{H}{r}\right)\right]\rho_w v_w \qquad (7)$$

where F_r^m is given in equation (3).

Conservation of momentum in the radial direction gives

$$\frac{\partial\,(2\pi r\,\Sigma_{bl}U)}{\partial t} + \frac{\partial\,(4\pi r\,F_r^p)}{\partial r} = 4\pi r^2\left[\frac{d}{dr}\left(\frac{H}{r}\right)\right]\rho_w {v_w}^2, \qquad (8)$$

where F_r^p is given in equation (3) and $U(r, t)$ in equation (4). The term $\partial(2\pi r\,\Sigma_{bl}U)/\partial t$ can be neglected because $\Sigma_{bl} \ll \Sigma_d$. Equation (8) can then be integrated from the inner radius of the disc r_{in} where $F_r^m = 0$ to a radius r to give

$$r\,F_r^m = \frac{\dot{M}_w v_w}{4\pi U}\left[\frac{H}{r} - \left(\frac{H}{r}\right)_i\right], \qquad (9)$$

where the i-subscript indicates evaluation at $r = r_{in}$. We have again assumed for simplicity that the stellar wind is spherically symmetric with both $\dot{M}_w = \text{const}$ and $v_w = \text{const}$ in space and time for $t > 0$. Thus, the right-hand side of equation (7) is

$$\mathcal{R}_{10} = -\dot{M}_w\frac{\partial}{\partial r}\left(\frac{v_w}{U}\left[\frac{H}{r} - \left(\frac{H}{r}\right)_i\right] - \frac{H}{r}\right). \qquad (10)$$

Equation (7) can be integrated using the method of characteristics. In view of the fact that $u = \text{const}$, we have

$$\frac{d(2\pi r\,\Sigma_d)}{dt} = \left(\frac{\partial}{\partial t} - u\frac{\partial}{\partial r}\right)(2\pi\Sigma_d). \qquad (11)$$

The characteristics are $r = r_0 - ut$, where r_0 is the radius of the disc fluid element at $t = 0$ with $r_{in} \le r_0 \le r_{out}$ and r_{out} the outer radius of the disc. At $t = 0$ the surface density of the disc is $\Sigma_{d0} = \Sigma_{0i}(r_{in}/r)$. Hence

$$\frac{d\hat{\Sigma}_d}{dt} = \frac{\mathcal{R}_{10}}{2\pi r_{in}\Sigma_{0i}}, \qquad (12)$$

where $\hat{\Sigma}_d(r, t) \equiv \Sigma_d(r, t)/\Sigma_{d0}(r)$. Integrating this equation gives

$$\begin{aligned}\hat{\Sigma}_d(r, t) &= 1 + \int_0^t dt\,\frac{\mathcal{R}_{10}}{2\pi r_{in}\Sigma_{0i}},\\ &= 1 + \int_r^{r+ut} dr'\,\frac{\mathcal{R}_{10}(r')}{2\pi r_{in} u\,\Sigma_{0i}},\\ &= 1 - F(r + ut) + F(r), \end{aligned} \qquad (13)$$

where

$$F(r) = \frac{\dot{M}_w}{\dot{M}_{d0}}\left(\frac{v_w}{U(r)}\left[\frac{H}{r} - \left(\frac{H}{r}\right)_i\right] - \frac{H}{r}\right), \qquad (14)$$

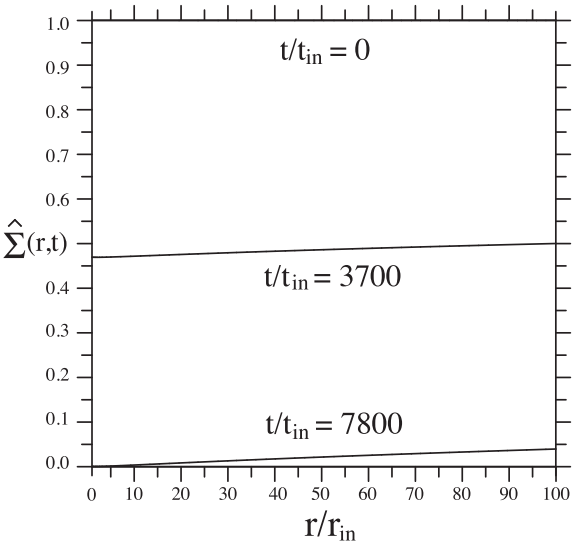

Figure 3. Evolution of the disc surface density $\hat{\Sigma}_d(r, t) = \Sigma_d(r, t)/\Sigma_d(r, 0)$ for an illustrative case discussed in the text. The radius is measured in units of the initial inner radius of the disc, $r_{in}(t = 0)$, which is taken to be $10r_\odot = 7 \times 10^{11}$ cm. Time is measured in units of $t_{in} = r_{in}/u = 257$ yr, where the accretion speed is $u = 86.3$ cm s^{-1} corresponding to a viscosity coefficient $\alpha = 10^{-2}$ and a disc half-thickness at r_{in} of $h_{in} = 0.025r_{in}$. Additionally, we have assumed $H/r = 0.03(r/r_{in})^\beta$ with $\beta = 0.3$ so that $(H/r)_{out} = 0.3$. Also, $U(r) = g(2GM/r)^{1/2}$ with $g = 2$ and $M = M_\odot$, which is twice the local escape speed.

with $\dot{M}_{d0} = 2\pi r_{in}\Sigma_{d0} = \text{const}$ being the disc accretion rate at the inner radius of the disc assuming the disc extents into $r_{in}(t = 0)$. As discussed in Section 3, we consider the mean boundary layer velocity U to be a factor $g \ge 1$ times larger than the local escape velocity; that is, $U(r) = g(2\,GM/r)^{1/2}$. Additionally, we assume $H/r = (H/r)_i(r/r_i)^\beta$ with $\beta > 1/4$.

An estimate of the time t_{cr} at which $\hat{\Sigma}$ decreases to zero at $r_{in}(t = 0)$ follows from equations (13) and (14) assuming $ut \gg r_{in}$,

$$t_{cr} \approx \frac{r_{in}(0)}{u}\left(\frac{\dot{M}_{d0}\; g\sqrt{2}\; v_{Ki}}{\dot{M}_w\;(H/r)_i\; v_w}\right)^{\frac{1}{\beta+1/2}}. \qquad (15)$$

Formally, t_{cr} is independent of r_{in}. The dominant factors determining this time-scale are u and $[v_w\dot{M}_w/(v_{Ki}\dot{M}_{d0})]$ with, for example, $t_{cr} \propto u^{-1}[v_{Ki}\dot{M}_{d0}/(v_w\dot{M}_w)])^{1.43}$ for $\beta = 0.3$. The physical interpretation of equation (15) is that the time-scale t_{cr} is larger than viscous accretion time-scale $r_{in}(0)/u$ by a dimensionless factor which scales as a fractional power of the ratio of the momentum flux of the expelled disc matter $\dot{M}_d v_K$ to the momentum flux of the wind $\dot{M}_w v_w$.

Fig. 3 shows the behaviour of $\hat{\Sigma}(r, t)$ for an illustrative case where (1) $t > 0$, (2) the stellar wind has $\dot{M}_w = 10^{-10}\,M_\odot$ yr^{-1} and $v_w = 10^3$ km s^{-1}, (3) the initial disc accretion rate is $\dot{M}_{d0} = 10^{-8}\,M_\odot$ yr^{-1}, and (4) the viscosity coefficient is $\alpha = 0.01$. A central hole in the disc appears at $t/t_{in} \approx 7.8 \times 10^3$ when $\hat{\Sigma}(r_{in}, t) = 0$ at $t \approx 2 \times 10^6$ yr which is approximately equal to t_{cr} of equation (15).

After a hole starts to form for $t > t_{cr}$, we can rewrite the normalizations to r_{in} in terms of normalizations to $r_{out} = \text{const}$. For example, $H/r = (H/r)_{out}(r/r_{out})^\beta$. In this way, we find for $t > t_{cr}$,

$$\frac{r_{hole}(t)}{r_{in}(0)} \approx 1 + 0.56\left(\frac{t - t_{cr}}{t_{in}}\right)^{1.25}, \qquad (16)$$

where $t_{in} = r_{in}(0)/u$. Evidently, the hole expands rapidly for $t > t_{cr}$.

4 INFLUENCE OF CMEs

The foregoing has considered disc erosion by a steady stellar wind. Note however that significant disc erosion can arise the episodic component of the stellar wind, namely, from frequent powerful CMEs. Recent Kepler data provided new insights on the properties of stellar activity in magnetically active stars. Specifically, they show the occurrence rates of flares with energies greater 10^{34} erg referred to as *superflares*. The data indicate that the occurrence rate of superflares from G-type stars follow the power-law relation with the flare's energy $E_{\rm f}$ as

$$\frac{{\rm d}N}{{\rm d}E_{\rm f}} = kE_{\rm f}^{-\alpha} \ \ {\rm events\,s^{-1}}, \tag{17}$$

where $\alpha \approx 2.1$ and $k \approx 2.7 \times 10^{32}$ in cgs units (Aarnio, Matt & Stassun 2013). This characterization of stellar activity is important not only in terms of understanding the total radiative output from young stars, but also in terms of the mass output in the form of CMEs that usually accompany solar flares. CMEs cannot be directly observed from other solar-like stars except for possible type III and type IV bursts at decametre wavelength introduced by accelerated electrons as a CME propagates out from the solar/stellar corona (Boiko et al. 2012; Konovalenko et al. 2012; Massi et al. 2013). However, the frequency of CMEs from the young Sun and other active stars can be estimated from their association with solar/stellar flares. Recent *SOHO*/ Large Angle and Spectrometric Coronagraph Experiment (LASCO) and *STEREO* observations of energetic and fast ($\gtrsim$500 km s^{-1}) CMEs from the Sun show strong association with powerful solar flares (Yashiro & Gopalswamy 2009; Aarnio et al. 2011). This empirical correlation provides a direct way to characterize CME frequencies of occurrence from statistics of solar and stellar flares via equation (17). The total ejected mass in each solar CME scales with the energy of the associated flare emitted in X-rays as

$$M_{\rm CME} = (2.7 \pm 1.2) \times 10^{-3} E_{\rm f}^{\beta} \ \ {\rm g}, \tag{18}$$

where $\beta \approx 0.63$ and $k_M \approx 2.7 \times 10^{-3}$ in cgs units (Aarnio et al. 2011). The solar CME masses vary between 10^{15} and 5×10^{16} g and contributes about 4 per cent of the total mass loss due to the solar wind.

If we extrapolate this relation to stellar superflares on young stars with the maximum energy of $E = 10^{36}$ erg, then the ejected mass per single event in a T Tauri star can be obtained by integrating equation (18) over the occurrence rate from equation (17) as

$$\dot{M}_{\rm CME} = \int_{E_{\rm min}}^{E_{\rm max}} {\rm d}E_{\rm f} M(E_{\rm f}) \frac{{\rm d}N}{{\rm d}E_{\rm f}}, \tag{19}$$

where $E_{\rm min,max}$ are discussed by Aarnio et al. (2013). Given the uncertainty of the power-law index α in equation (17), the calculated mass-loss rate due to CMEs is $\sim$(3–10) $\times 10^{-10}\,{\rm M}_{\odot}\,{\rm yr}^{-1}$ (Aarnio et al. 2013; Drake et al. 2013).

The disc erosion rate due to sporadic high-velocity CMEs with $\dot{M}_{\rm CME}$ comparable to the above considered steady wind $\dot{M}_{\rm w}$ is expected to be similar to the steady disc erosion rate. A CME impacting the disc at a distance r with momentum $M_{\rm CME} v_{\rm CME}$ can eject disc matter $\Delta M_{\rm d}$ with momentum $\Delta M_{\rm d}\, v_{\rm esc}(r)$.

5 CONCLUSIONS

This work develops an analytic model of protodiscs' gas and entrained dust erosion due to high-velocity magnetized stellar winds. The presence of the magnetic field leads to Reynolds numbers sufficiently large to cause a strongly turbulent wind/disc boundary layer. This boundary layer entrains and carries away the disc gas and entrained dust. Strong magnetized winds from young stars ($\lesssim 10^7$ yr) with discs are likely because the stars are known to rotate rapidly and to be strongly magnetized. The analytic model assumes a steady stellar wind with mass-loss rate $\dot{M}_{\rm w} \sim 10^{-10}\,{\rm M}_{\odot}\,{\rm yr}^{-1}$ and velocity $v_{\rm w} \sim 10^3$ km s^{-1}. However, in Section 4, we discuss the contribution to the disc erosion due to frequent powerful CMEs where the average mass-loss rate in CMEs ($\dot{M}_{\rm CME}$) and velocities ($v_{\rm CME}$) have values comparable to those for the steady wind.

Sample results for the evolution of the disc surface density $\hat{\Sigma}_{\rm d} = \Sigma_{\rm d}(r,t)/\Sigma(r,0)$ are shown in Fig. 3. The inner region of the disc surface density decreases more rapidly than that at larger radii with the result that a hole forms after a critical time $t_{\rm cr}$. For the case shown, this time is about 2×10^6 yr. The critical time is proportional to the inverse accretion speed in the disc u = const times the ratio $\dot{M}_{\rm d0}/\dot{M}_{\rm w}$ raised to a power larger than unity, where $\dot{M}_{\rm d0}$ is the initial disc accretion rate and $\dot{M}_{\rm w}$ is the mass-loss rate in the wind. The radius of the hole expands continuously with time. This is an important difference between wind erosion and photoevaporation models where the inner hole is typically less than 10 au (Owen, Ercolano & Clarke 2011). The possible role of wind erosion for transition discs is complicated by the likely presence of one or more planets at radii $\lesssim$10 au (Espaillat et al. 2014). More realistic models would have u dependent on space and time, and $v_{\rm w}$ and $\dot{M}_{\rm w}$ dependent on time as the star spins down.

The stellar wind disc erosion in the presence of a radially distributed magnetocentrifugal disc wind (Blandford & Payne 1982) remains to be investigated. One possibility is that any radially distributed poloidal magnetic field initially threading the disc is advected inwards to the disc/magnetosphere boundary where it gives rise to a steady X-wind (Shu et al. 1994) or to the episodic conical wind outflows found in *global* MHD simulations (e.g. Romanova et al. 2009; Lii et al. 2012, 2014; Dyda et al. 2013; Zanni & Ferreira 2013). During the intervals when the conical wind is 'off', the stellar wind can flow freely and impact the disc. Another possibility is that a radially distributed poloidal field $B_{\rm p}(r)$ exists out to $r \gtrsim 10$ au for the disc lifetime and gives rise to magnetically driven winds as found in the MHD shearing box simulations of Bai & Stone (2013a,b). The mass-loss in these winds could provide another mechanism for disc dispersal (Armitage, Simon & Martin 2013). The stellar wind erosion discussed here is expected to dominate the magnetic disc winds if the ram pressure of the wind $\rho_{\rm w} v_{\rm w}^2$ is larger than $B_{\rm p}^2/8\pi$.

ACKNOWLEDGEMENTS

We thank Professor J. P. Lloyd for helpful discussions and an anonymous referee for valuable criticism and suggestions on an earlier version of this work. This work was supported in part by NASA grants NNX11AF33G, NNX12AI85G, and NSF grant AST-1211318.

REFERENCES

Aarnio A. N., Stassun K. G., Hughes W. J., McGregor S. L., 2011, Sol. Phys., 268, 195
Aarnio Matt S. P., Stassun K. G., 2013, Astron, Nachr., 334, 77
Andrews S. M., Williams J. P., 2005, ApJ, 631, 1134
Armitage P. J., 2010, The Astrophysics of Planet Formation. Cambridge Univ. Press, New York
Armitage P. J., Clarke C. J., 1996, MNRAS, 280, 458
Armitage P. J., Simon J. B., Martin R. G., 2013, ApJ, 778, L14
Bai X.-N., Stone J. M., 2013a, ApJ, 767, 30
Bai X.-N., Stone J. M., 2013b, ApJ, 769, 76
Belcher J. W., MacGregor K. B., 1976, ApJ, 210, 498

Birnstiel T., Pinilla P., Andrews S. M., Benisty M., Eercolano B., 2013, in Barge P., Jorda L., eds, EPJ Web Conf., Instabilities and Structures in Proto-Planetary Disks. p. 46
Blandford R. D., Payne D. G., 1982, MNRAS, 199, 883
Boiko A. I., Melnik V. N., Konovalenko A. A., Abranin E. P., Dorovskyy V. V., Rucker H. O., 2012, Adv. Astron. Space Phys., 2, 76
Bouvier J., Cabrit S., Fernández M., Martín E. L., Matthews J. M., 1993, A&A, 272, 176
Bouvier J., Matt S. P., Scholz A., Stassun K. G., Zanni C., 2014, in Beuther H., Klessen R., Dullemond K., Henning Th., eds, Protostars & Planets VI. Univ. Arizona Press, Tucson, AZ, p. 22
Braginskii S. I., 1965, Review of Plasma Physics, Vol. 1. Consultants Bureau, New York
Clarke C. J., Gendrin A., Sotomayor M., 2001, MNRAS, 328, 485
Drake J. J., Cohen O., Yashiro S., Gopalswamy N., 2013, ApJ, 764, 170
Dyda S., Lovelace R. V. E., Ustyugova G. V., Lii P. S., Romanova M. M., Koldoba A. V., 2013, MNRAS, 432, 127
Espaillat C. et al., 2007, ApJ, 664, L111
Espaillat C. et al., 2014, in Beuther H., Klessen R., Dullemond K., Henning Th., eds, Protostars & Planets VI. Univ. Arizona Press, Tucson, AZ, p. 24
Hartmann L., Calvet N., Gullbring E., D'Alessio P., 1998, ApJ, 495, 385
Hollenbach D. J., Yorke H. W., Richstone D., 2000, in Mannings V., Boss A. P., Russell S. S., eds, Protostars and Planets IV. Univ. Arizona Press, Tucson, AZ, p. 406
Johns-Krull C. M., 2007, ApJ, 664, 975
Johns-Krull C. M., Valenti J. A., 2000, in Pallavicini R., Micela G., Sciortino S., eds, ASP Conf. Ser. Vol. 198, Stellar Clusters and Associations: Convection, Rotation, and Dynamos. Astron. Soc. Pac., San Francisco, p 371
Königl A., 1991, ApJ, 370, L39
Konovalenko A. A. et al., 2012, European Planetary Science Congress, Vol. 7, Planetary, Solar and Exoplanetary Radio Emissions. id. EPSC2012-902 2012
Lii P., Romanova M. M., Lovelace R. V. E., 2012, MNRAS, 4200, 2020
Lii P., Romanova M. M., Ustyugova G. V., Koldoba A. V., Lovelace R. V. E., 2014, MNRAS, 441, 86
Long M., Romanova M. M., Lovelace R. V. E., 2005, ApJ, 634, 1214
Lovelace R. V. E., Romanova M. M., Bisnovatyi-Kogan G. S., 1999, ApJ, 514, 368
Lovelace R. V. E., Romanova M. M., Barnard A. W., 2008, MNRAS, 389, 1233
Massi M., Ros E., Boboltz D., Menten K. M., Neidhfer J., Torricelli-Ciamponi G., Kerp J., 2013, Mem. Soc. Astron. Ital., 84, 359
Matt S., Pudritz R. E., 2008a, ApJ, 678, 1109
Matt S., Pudritz R. E., 2008b, ApJ, 681, 391
Michel F. C., 1969, ApJ, 158, 727
Owen J. E., Ercolano B., Clarke C. J., 2011, MNRAS, 412, 13
Owen J. E., Clarke C. J., Ercolano B., 2012, MNRAS, 422, 1880
Piétu V., Dutrey A., Guilloteau S., Chapillon E., Pety J., 2006, A&A, 430, L43
Regály Zs., Juhsz A., Sndor Zs., Dullemond C. P., 2012, MNRAS, 419, 1701
Richling S., Yorke H. W., 1997, A&A, 324, 317
Romanova M. M., Ustyugova G. V., Koldoba A. V., Lovelace R. V. E., 2005, ApJ, 635, L165
Romanova M. M., Ustyugova G. V., Koldoba A. V., Lovelace R. V. E., 2009, MNRAS, 399, 1802
Roy C. J., Blottner F. G., 2006, Prog. Aerosp. Sci., 42, 469
Schlichting H., 1968, Boundary-Layer Theory. McGraw-Hill, New York, ch. 23
Shakura N. I., Sunyaev R. A., 1973, A&A, 24, 337
Shu F., Najita J., Ostriker E., Wilkin F., Ruden S., Lizano S., 1994, ApJ, 429, 781
Skrutskie M. F., Dutkevitch D., Strom S. E., Edwards S., Strom K. M., 1990, AJ, 99, 1187
Ustyugova G. V., Koldoba A. V., Romanova M. M., Lovelace R. V. E., 2006, ApJ, 646, 304
Weber E. J., Davis L., 1967, ApJ, 148, 217
Wolk S. J., Walter F. M., 1996, AJ, 111, 2066
Yashiro S., Gopalswamy N., 2009, in Gopalswamy N., Webb D. F., eds, Proc. IAU Symp. 257, Universal Heliophysical Processes. Cambridge Univ. Press, Cambridge, p. 233
Zanni C., Ferreira J., 2013, A&A, 550, A99
Zsom A., Ormel C. W., Güttler C., Blum J., Dullemond C. P., 2010, A&A, 513, A57

This paper has been typeset from a TEX/LATEX file prepared by the author.